VALIDATION OF 3D LEFT VENTRICULAR DEFORMATIONS PREDICTED BY HYPERELASTIC WARPING AND CINE-MRI

Alexander I. Veress, Jeffrey A. Weiss, Gregory J. Klein, Grant T. Gullberg

Post-doctoral Fellow
Department of Bioengineering
University of Utah, Salt Lake City, Utah

Assistant Professor
Department of Bioengineering
University of Utah, Salt Lake City, Utah

Scientist
Department of Medicine and Functional Imaging
E. O. Lawrence Berkeley National Laboratory,
Berkeley, California

Senior Scientist
Department of Medicine and Functional Imaging
E. O. Lawrence Berkeley National Laboratory,
Berkeley, California

INTRODUCTION

Assessment of regional heart wall deformation (wall motion, thickening, strain) can provide quantitative information regarding ventricular wall function, can localize ischemic myocardial disease and can identify impairment of cardiac function due to hypertrophic or dilated cardiomyopathies. Our long-term goal is to improve the diagnosis and treatment of these pathologies by developing validated techniques that will allow determination of the changes in strain distribution resulting from these conditions.

We have developed an image based finite element technique known as Warping that allows the extraction of strain information from sequences of images of a deforming tissue without markers [2] or the necessity of using tagged Magnetic Resonance Imaging (MRI) [1]. While MRI tagging techniques allow non-invasive measurements of myocardial wall dynamics [1], major limitations for cardiac imaging are its spatial resolution, which is much coarser than the MRI acquisition matrix, and the lengthy acquisition time. The present work addresses the validation of use of Warping with cine MRI data to determine fiber stretch distribution in the left ventricle during the cardiac cycle through the comparison of Warping results from an image data set where the exact strains and displacements were known. Additionally, a parameter study was performed to determine the sensitivity of the Warping analysis to changes in material parameters.

METHODS

Hyperelastic Warping: A brief description of the Warping technique for deformable image registration is provided below. Additional details can be found in previous publications [2,3]. The approach requires an image of the tissue in a reference configuration (*template* image), and an image in the deformed configuration (*target* image). The Warping technique produces a position-dependent body force from the pointwise intensity differences between pairs of image datasets. The body force is applied to a finite element (FE) representation of the object of interest in the template image domain, causing it to deform into registration with the target image. The Warping body force is derived from the pointwise difference in intensities and intensity gradients between the template and target images.

Gated cine MRI images of a normal volunteer's heart were acquired during end-systole on a 1.5T Siemens scanner (256x256 image matrix, 378 mm FOV, 10 mm slice thickness, 10 slices). The volumetric MRI dataset corresponding to end-systole was designated as the template image. The target image dataset corresponding to end-diastole was created as detailed below.

Finite Element Model Generation: The 2D contours of the left ventricular endocardial and epicardial surfaces were segmented manually from the end-systolic MRI image datasets and then imported into a commercial mesh generation package to create the FE models. The myocardium was represented as a transversely isotropic material with the fiber angle varying from -90^o at the epicardial surface, through 0^o at the mid-wall, to 90^o at the endocardial surface. The material coefficients were determined by least squares fit of the transversely isotropic hyperelastic constitutive model described in Weiss et al. [4] to the biaxial stress/strain values presented in the work of Humphrey et al. [5]. The uniaxial form of the constitutive equation takes the form

$$\sigma = C_1\left(\lambda^2 - \frac{1}{\lambda}\right) + C_2\left(\lambda - \frac{1}{\lambda^2}\right) + \lambda W_\lambda \qquad (1)$$

Here, σ is the uniaxial Cauchy stress, λ is the stretch along the fiber direction, C_1 and C_2 are material coefficients, and W_λ is the fiber family strain energy function, defined as

$$\lambda W_\lambda = 0, \qquad \lambda < 1,$$
$$\lambda W_\lambda = C_3\left[\exp\left(C_4(\lambda - 1)\right) - 1\right], \qquad \lambda \geq 1.$$

The material coefficients C_3 and C_4 scale the fiber stress and control its rate of rise with increasing stretch, respectively.

An internal pressure load was applied to the endocardial surface of the FE model until the strain distribution corresponded to that found in the literature [6] and was analyzed using the NIKE3D finite

element program [7]. The template end-diastolic image was created by mapping the end-systolic image using the displacement values determined from the forward solution of the pressure-loaded FE model. This created a target image where the exact strains and displacements are known. A Warping analysis was then performed using the two image datasets. The fiber stretch results of the forward and Warping solutions were compared. To determine the sensitivity of the Warping analysis to changes in material parameters, C_1 and C_3 were increased and decreased by 24% of the baseline values. The 24% increase and decrease corresponds to the 95% confidence interval of material parameters determined from the least-squares fit of the material model to the Humphrey et al. data. The forward and Warping sensitivity study results were compared at eight locations (Figure 1).

RESULTS

The overall results for fiber stretch demonstrated good agreement between the forward and the Warping distributions (Figure 1). A detailed analysis of the forward and Warping nodal stretch distributions for each image plane indicates excellent agreement, with the best correlation on the mid-axial planes (Figure 2). The sensitivity results are given in Table 1.

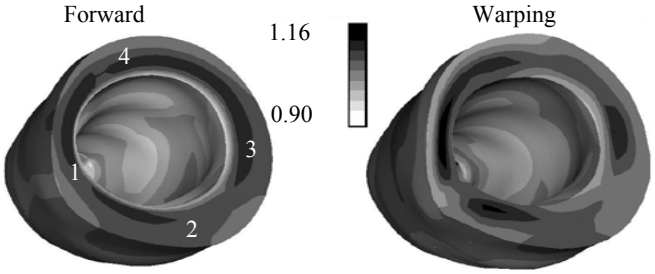

Figure 1. Fiber stretch distribution for the forward (left) and warping (right) analyses. The locations for the sensitivity analysis are shown on the forward model as numbers 1-4. Locations 5-8 are at the same locations as 1-4 but at the mid-ventricle level.

Location	1	2	3	4	5	6	7	8
Forward	1.09	1.06	1.12	1.07	1.08	1.04	1.02	1.05
C_1+24%	1.09	1.09	1.13	1.07	1.07	1.03	1.03	1.05
C_1-24%	1.09	1.09	1.13	1.07	1.08	1.03	1.03	1.05
C_3+24%	1.09	1.08	1.13	1.08	1.08	1.03	1.03	1.05
C_3-24%	1.10	1.09	1.13	1.07	1.08	1.03	1.03	1.05

Table 1: Effect of changes in material properties on predicted fiber stretch.

DISCUSSION

The results of this study demonstrate that Warping can accurately predict the stretch distributions from cine MRI images for a case when the exact solution is known. The sensitivity results indicate that the Warping analysis is relatively insensitive to material parameters over the range of values found in the literature. This insensitivity to material parameters allows for the analysis of material where the exact material properties are unknown. Furthermore, previous work has shown that knowledge of the exact material model is not necessary in order to determine accurate strain/displacement results.

Warping has two advantages over tagged MRI analyses. First, it provides a higher spatial resolution than tagged analysis. Second, untagged MRI datasets require a shorter acquisition time than required for a full 3-D tagged image dataset. This is a distinct advantage for analysis of patients with myocardial damage, since the length of time that they can lie supine is very limited.

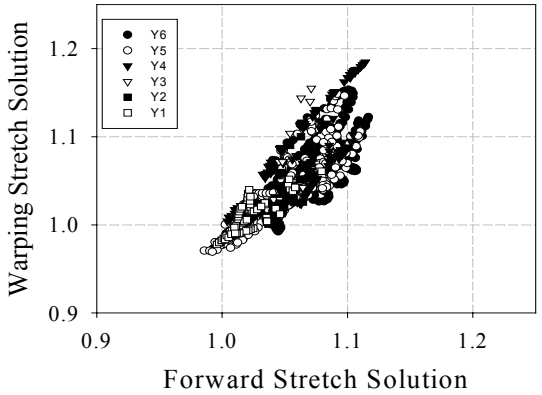

Figure 2. Comparison of Warping and forward nodal stretch values for each image slice. Y7 corresponds to the slice at the base of the LV and Y1 is near the apex of the heart.

The present work has several limitations. The slice thickness used was relatively large (10 mm). This may contribute to errors in the Warping predictions. Second, validation was performed using ideal, noiseless image datasets for which the exact solution was known. These issues can be addressed by using higher-resolution image acquisition parameters and validating the Warping technique against predictions obtained via MRI tagging. We are currently working on performing these direct comparisons. Nevertheless, the results of this study demonstrate that Warping can be used with Cine MRI data to provide estimates of fiber stretch in the ventricular wall. This will allow high-resolution noninvasive measurement provides of ventricular deformation without MRI tagging techniques.

REFERENCES

[1] Ozturk, C. and McVeigh, E. R., 2000. "Four-Dimensional B-Spline Based Motion Analysis of Tagged MR Images: Introduction and in Vivo Validation," Phys Med Biol, Vol. 45, No. 6, pp. 1683-702.

[2] Weiss, J. A., Rabbitt, R. D., and Bowden, A. E., 1998. "Incorporation of Medical Image Data in Finite Element Models to Track Strain in Soft Tissues," SPIE, Vol. 3254, pp. 477-484.

[3] Rabbitt, R. D., Weiss, J. A., Christensen, G. E., and Miller, M. I., 1995. "Mapping of Hyperelastic Deformable Templates Using the Finite Element Method.," SPIE, Vol. 2573, pp. 252-265.

[4] Weiss, J. A., Maker, B. N., and Govindjee, S., 1996. "Finite Element Implementation of Incompressible, Transversely Isotropic Hyperelasticity," Comput Methods Appl Mech Eng, Vol. 135, pp. 107-128.

[5] Humphrey, J. D., Strumpf, R. K., and Yin, F. C., 1990. "Determination of a Constitutive Relation for Passive Myocardium: I. A New Functional Form," J Biomech Eng, Vol. 112, No. 3, pp. 333-9.

[6] Tseng, W. Y., Reese, T. G., Weisskoff, R. M., Brady, T. J., and Wedeen, V. J., 2000. "Myocardial Fiber Shortening in Humans: Initial Results of Mr Imaging," Radiology, Vol. 216, No. 1, pp. 128-39.

[7] Maker, B. N., Ferencz, R. M., and Hallquist, J. O., 1990. "NIKE3D: A Nonlinear Code for Solid and Structural Mechanics.," Lawrence Livermore National Laboratories Technical Report UCRL-MA-105208, Rev 1.